CALT-TH-2017-063
FERMILAB-PUB-17-400-T

Power Corrections to the Universal Heavy WIMP-Nucleon Cross Section

Chien-Yi Chen[1,2], Richard J. Hill[3,4], Mikhail P. Solon[5], and Alexander M. Wijangco[6]

[1] *Department of Physics and Astronomy, University of Victoria, Victoria, BC V8P 5C2 Canada*
[2] *Perimeter Institute for Theoretical Physics, Waterloo, ON, N2L 2Y5 Canada*
[3] *Department of Physics and Astronomy, University of Kentucky, Lexington, KY 40506, USA*
[4] *Fermilab, Batavia, IL 60510, USA*
[5] *Walter Burke Institute for Theoretical Physics, California Institute of Technology, Pasadena, CA 91125, USA*
[6] *TRIUMF, Vancouver, BC, V6T 2A3 Canada*

January 25, 2018

Abstract

WIMP-nucleon scattering is analyzed at order $1/M$ in Heavy WIMP Effective Theory. The $1/M$ power corrections, where $M \gg m_W$ is the WIMP mass, distinguish between different underlying UV models with the same universal limit and their impact on direct detection rates can be enhanced relative to naive expectations due to generic amplitude-level cancellations at leading order. The necessary one- and two-loop matching calculations onto the low-energy effective theory for WIMP interactions with Standard Model quarks and gluons are performed for the case of an electroweak SU(2) triplet WIMP, considering both the cases of elementary fermions and composite scalars. The low-velocity WIMP-nucleon scattering cross section is evaluated and compared with current experimental limits and projected future sensitivities. Our results provide the most robust prediction for electroweak triplet Majorana fermion dark matter direct detection rates; for this case, a cancellation between two sources of power corrections yields a small total $1/M$ correction, and a total cross section close to the universal limit for $M \gtrsim \text{few} \times 100\,\text{GeV}$. For the SU(2) composite scalar, the $1/M$ corrections introduce dependence on underlying strong dynamics. Using a leading chiral logarithm evaluation, the total $1/M$ correction has a larger magnitude and uncertainty than in the fermionic case, with a sign that further suppresses the total cross section. These examples provide definite targets for future direct detection experiments and motivate large scale detectors capable of probing to the neutrino floor in the TeV mass regime.

1 Introduction

The WIMP paradigm remains a leading explanation for astrophysical dark matter. Null results at the LHC [1–4] suggest that new physics is heavy compared to masses of weak scale particles, $\sim 100\,\text{GeV}$. This situation presents experimental challenges. For example, at high-energy colliders it is difficult to produce and detect on-shell heavy states that are coupled weakly to the Standard Model. Production cross sections are small and novel search strategies are required to distinguish signal from background. For the $SU(2)_W \times U(1)_Y$ charged WIMPs considered in this paper, with masses above the electroweak scale, detection prospects remain challenging at foreseeable colliders [5–10]. Indirect searches for WIMP annihilation signals present a complementary set of opportunities and experimental challenges, and introduce dependence on astrophysical modeling [11–18]. Heavy particle techniques can be similarly applied to this case [15, 19–21].

The heavy WIMP regime is also challenging for direct detection prospects. First, since the abundance of astrophysical dark matter particles for a given local energy density scales inversely as the particle mass, WIMPs are less abundant and detection rates for a given cross section are smaller. Second, as the mass spectrum of new physics states becomes stretched above the weak scale, the absence of accessible intermediate states forbids the simplest higgs-mediated interactions of WIMPs with nucleons, causing cross sections to be smaller.

However, although the interaction rates between WIMPs and nucleons may become smaller, they also become more certain. Heavy WIMP symmetry emerges in the limit that the WIMP mass, M, is large compared to the electroweak scale, i.e., $M \gg m_W$. Scattering cross sections become universal for given WIMP gauge quantum numbers, independent of the detailed UV physics [22, 23]. For example, the cross section in this limit is independent of whether the particle is scalar or fermion, composite or fundamental. This universality provides robust sensitivity targets for ambitious next generation direct detection experiments, and will be key to interpreting any confirmed signal.

In previous work, two of the authors (RJH and MPS) analyzed the universal heavy WIMP limit for WIMP-nucleon scattering [22–25]. In this limit a generic amplitude-level cancellation [22, 23, 26] was shown to suppress the low-velocity WIMP-nucleon cross section to the level of $\sim 10^{-47}\,\text{cm}^2$ for wino-like WIMPs (i.e., self-conjugate electroweak triplets), and higgsino-like cross sections to an even smaller value. It is natural to ask whether in the presence of such cancellations, formally subleading effects can become numerically relevant beyond naive dimensional estimates. For example, focusing on the electroweak triplet case, the cancellation results in a total amplitude whose magnitude is $\sim 20\%$ the size of the component subamplitudes [25], and a WIMP-nucleon cross section that is therefore suppressed by more than an order of magnitude. For TeV scale WIMPs, corrections of order m_W/M could potentially enter at a similar numerical level. Here we analyze such $1/M$ power corrections, and quantify the corresponding violations of heavy WIMP universality.

The remainder of the paper is structured as follows. Section 2 extends Heavy WIMP Effective Theory (HWET) to incorporate $1/M$ power corrections, and Sec. 3 matches to the low energy effective theory after integrating out weak-scale particles. Section 4 computes the low-velocity scattering cross section of WIMPs on nucleons. Section 5 provides a summary and outlook.

2 Heavy WIMP Effective Theory at order $1/M$

Heavy particle effective theory can be used to analyze Standard Model (SM) extensions consisting of electroweak multiplets whose mass M is large compared to SM particle masses, $M \gg m_W$. Additional heavy multiplets, of mass M', may be integrated out for generic mass splitting $M' - M = \mathcal{O}(M)$. The special case $M' - M = \mathcal{O}(m_W)$ requires that the additional multiplet appear explicitly in the HWET [23].[1]

[1] For a related application of heavy particle effective theory to the case of an electroweak singlet bino that is nearly degenerate with a stop, see Ref. [27].

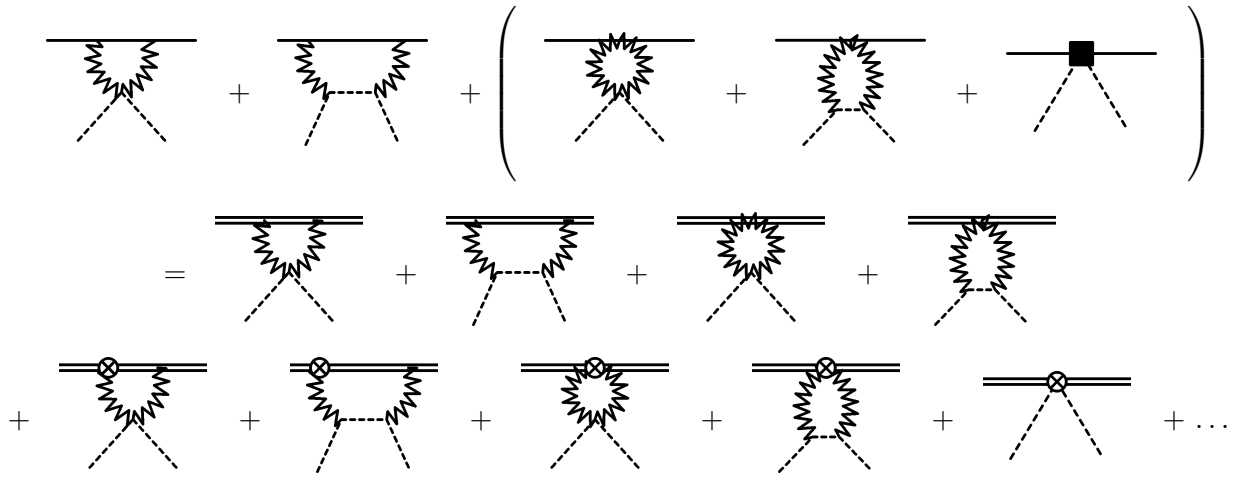

Figure 1: Matching condition for the coefficient c_H for UV theory consisting of the Standard Model plus $SU(2)_W$-triplet Majorana fermion. Solid lines denote Majorana fermion, dashed lines denote SM Higgs doublet, zigzag lines denote $SU(2)_W$ gauge fields. Matching is performed in the electroweak symmetric theory. Double lines on the RHS denote heavy WIMPs and the encircled cross denotes insertion of a $1/M$ effective theory vertex. For UV theory consisting of a composite real scalar transforming as a triplet under $SU(2)_W$, the additional bracketed terms appear on the LHS, including the counterterm contribution denoted by the solid square.

Here we focus on a single multiplet of self-conjugate heavy particle fields with arbitrary spin, transforming under irreducible representations of electroweak $SU(2)_W \times U(1)_Y$. Where a specific representation is required, we illustrate with an electroweak triplet.

Working through order $1/M$, the gauge- and Lorentz-invariant lagrangian in the one-heavy-particle sector (i.e., bilinear in h_v) is [22]

$$\mathcal{L} = \overline{h}_v \left\{ iv\cdot D - \delta m - \frac{D_\perp^2}{2M} + c_H \frac{H^\dagger H}{M} + c_{W1} \frac{\sigma^{\mu\nu} W_{\mu\nu}}{M} + c_{W2} \frac{\epsilon^{\mu\nu\rho\sigma} \sigma_{\mu\nu} W_{\rho\sigma}}{M} + \dots \right\} h_v \,, \tag{1}$$

where the timelike unit vector v^μ defines the heavy WIMP velocity, $D_\mu = \partial_\mu - ig_1 Y B_\mu - ig_2 W_\mu^a t^a$ is the covariant derivative, $W_{\mu\nu} = i[D_\mu, D_\nu]/g_2 = W_{\mu\nu}^a t^a$ is the field strength, and $D_\perp^\mu = D^\mu - v^\mu v\cdot D$. The heavy particle field h_v satisfies projection relations as discussed in detail in Ref. [28]; for example, a fermionic heavy particle field obeys $\not{v} h_v = h_v$. The self-conjugate condition is enforced in the effective theory by requiring invariance of the lagrangian under

$$v^\mu \to -v^\mu \,, \quad h_v \to h_v^c \,, \tag{2}$$

where h_v^c denotes charge conjugation. For an irreducible representation of a self-conjugate field, we necessarily have zero hypercharge and integer isospin. The interactions labeled by c_{W1} and c_{W2} are present for the fermionic case. They contribute only to spin-dependent interactions at low velocity and will be ignored in the following.

The coefficient, $-1/2$, of the kinetic term $D_\perp^2/M$ in Eq. (1) is fixed by relativistic invariance [28, 29]. The residual mass, δm in Eq. (1), may be chosen for convenience. In a theory without electroweak symmetry breaking, taking $\delta m = 0$ would enforce that M is the physical particle (pole) mass. For matching calculations at the electroweak scale, it is convenient to choose $\delta m = c_H \langle |H|^2 \rangle / M$ to cancel the mass contribution from electroweak symmetry breaking.

The parameter c_H encodes ultraviolet physics above the scale M, and can be determined by a matching computation between a specified UV theory and HWET, described by Eq. (1). As an example, let

us consider the case where the UV theory is given by the SM and an electroweak triplet of Majorana fermions. Matching onto HWET is illustrated in Fig. 1. The matching can be performed in the electroweak symmetric theory. After expanding in the Higgs mass parameter, the EFT diagrams are scaleless but dimensionful and thus vanish in dimensional regularization. Evaluation of the full theory diagrams yields the matching condition,

$$c_H(\text{Majorana fermion}) = -3\alpha_2^2\,. \tag{3}$$

As a simple renormalizable extension of this case, consider an additional electroweak multiplet transforming with higgsino quantum numbers ($\mathrm{SU}(2)_W$ doublet, hypercharge $Y = 1/2$) with mass M_D. For generic doublet-triplet mass splitting, $M_D - M_T = \mathcal{O}(M_T)$, the matching coefficient becomes

$$c_H(\text{doublet} - \text{triplet}) = -3\alpha_2^2 + 4\pi\alpha_2\kappa^2\frac{M_T}{M_D - M_T}\,, \tag{4}$$

where κ is the renormalizable trilinear coupling between the triplet and doublet fermions and the SM Higgs field [23, 24]. As expected, when $M_D/M_T \to \infty$, the result (4) reduces to the pure triplet result (3).

As an example involving scalar versus fermionic WIMP, consider the pseudo-Goldstone bosons that emerge from a QCD-like SM extension with vector-like $\mathrm{SU}(2)_W$ couplings to underlying fermions [30, 31]. Recall that the lightest such states form an electroweak triplet, regardless of the fermionic $\mathrm{SU}(2)_W$ representation, and these "weakly interacting stable pions" are stabilized by a discrete symmetry (the unbroken analog of Standard Model G parity) [31]. The matching is again illustrated in Fig. 1, where now the full theory diagrams involve relativistic scalars, and also a counterterm four point function between the WIMP and SM Higgs field. The one-loop diagrams are UV divergent as a function of the cutoff Λ_h representing the new strong interaction scale. The divergence is cancelled by the counterterm contribution. For the composite theory under consideration, the divergence corresponds to a logarithmically enhanced term in the matching. Taking this "chiral" logarithm as an estimate, we have

$$c_H(\text{composite scalar}) = \alpha_2^2\log\frac{\Lambda_h^2}{M^2} + \cdots \approx \alpha_2^2\log\frac{1}{\alpha_2} + \ldots\,, \tag{5}$$

where the ellipsis denotes $\mathcal{O}(1)$ terms that are not logarithmically enhanced. The last equality corresponds to a chiral symmetry breaking mass M induced by $\mathrm{SU}(2)_W$ radiative corrections: $M^2/\Lambda_h^2 \sim \alpha_2$ [31]. The precise matching condition could in principle be computed using strong interaction methods in the chosen UV theory.

The cases (3), (4), and (5) establish the range of c_H encountered in a variety of weakly coupled UV models, involving fermions and scalars, composite and elementary particles, and both pure-state and multi-component models. Before investigating the impact of these differences on direct detection cross sections, let us perform the remaining step of matching HWET onto effective QCD operators.

3 Effective Theory Below the Weak Scale

The scale separation $m_W \gg \Lambda_{\mathrm{QCD}}$, is exploited by matching onto a heavy particle effective theory for the relevant electrically neutral component of the WIMP, interacting with five flavor QCD:

$$\mathcal{L} = \overline{h}_v^{(0)} h_v^{(0)}\left\{\sum_{q=u,d,s,c,b}\left[c_q^{(0)}O_q^{(0)} + c_q^{(2)}v_\mu v_\nu O_q^{(2)\mu\nu}\right] + c_g^{(0)}O_g^{(0)} + c_g^{(2)}v_\mu v_\nu O_g^{(2)\mu\nu}\right\} + \ldots\,. \tag{6}$$

This matching step is common to different UV realizations of the electroweak triplet WIMP. In Eq. (6), $h_v^{(0)}$ is the neutral WIMP, and the spin-0 and spin-2 QCD operators for quarks and gluons are given by

$$O_q^{(0)} = m_q\bar{q}q\,, \qquad\qquad O_q^{(2)\mu\nu} = \frac{1}{2}\bar{q}\left(\gamma^{\{\mu}iD_-^{\nu\}} - \frac{g^{\mu\nu}}{d}i\not{D}_-\right)q\,,$$

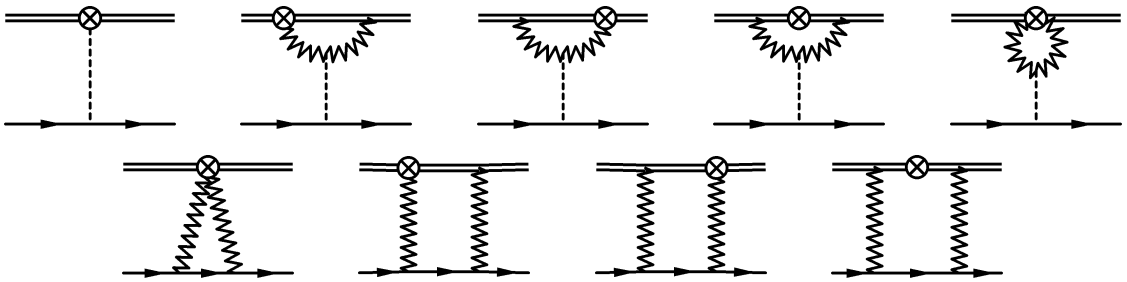

Figure 2: Diagrams contributing to $1/M$ quark matching, with the same notation as in Fig. 1. Diagrams with crossed W lines are not displayed.

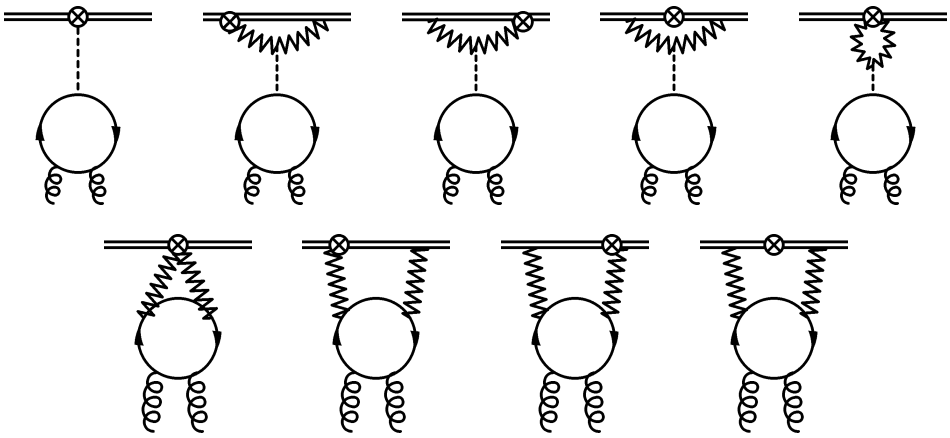

Figure 3: Diagrams contributing to $1/M$ gluon matching, with the same notation as in Fig. 1. Curly lines denote gluons. Diagrams with both gluons attached to the upper quark line or with one gluon attached to each of the upper and lower quark lines are not shown.

$$O_g^{(0)} = (G^A_{\mu\nu})^2\,, \qquad\qquad O_g^{(2)\mu\nu} = -G^{A\mu\lambda}G^{A\nu}_{\lambda} + \frac{1}{d}g^{\mu\nu}(G^A_{\alpha\beta})^2\,, \tag{7}$$

where $d = 4 - 2\epsilon$ is the spacetime dimension, $D_- \equiv \overrightarrow{D} - \overleftarrow{D}$, and curly braces denote symmetrization, $A^{\{\mu}B^{\nu\}} \equiv (A^\mu B^\nu + A^\nu B^\mu)/2$. The ellipsis in Eq. (6) denotes higher dimension operators suppressed by $\Lambda_{\rm QCD}/m_W$, and spin-dependent operators.

By restricting to dimension seven operators in Eq. (6), we are neglecting contributions suppressed by additional powers of $\Lambda^2_{\rm low-energy}/m_W^2$, where $\Lambda_{\rm low-energy}$ denotes any scale below m_W (e.g., m_b, or $\Lambda_{\rm QCD}$). However, we will account for corrections of order m_W/M in the coefficient functions appearing in Eq. (6) in our analysis of HWET power corrections. This power counting is appropriate for dark matter masses in the few hundred GeV to TeV range, a focus for current and next generation direct detection experiments.

We now proceed to match the theory (1) to the theory (6). By integrating out weak scale particles (the Higgs boson, electroweak gauge bosons, and the top quark), we obtain a solution for the twelve effective theory coefficients ($c_q^{(0)}$ and $c_q^{(2)}$ with $q = u, d, s, c, b$, as well as $c_g^{(0)}$ and $c_g^{(2)}$) that specify the interactions of DM with five flavor QCD. We neglect subleading corrections involving light quark masses, and use CKM unitarity to simplify sums over quark flavors. Approximating $|V_{tb}| \approx 1$, these simplifications imply that $c_u^{(S)} = c_d^{(S)} = c_s^{(S)} = c_c^{(S)}$ for $S = 0, 2$, leaving six independent coefficients. In the following, we denote generic up- and down-type quarks in five-flavor QCD by U and D, respectively, and an arbitrary quark flavor by q.

Feynman diagrams contributing to the matching at $\mathcal{O}(1/M)$ for the quark and gluon coefficients are shown in Figs. 2 and 3, respectively. Diagrams for gluon operators contain an additional loop compared to diagrams for quark operators. However, owing to the large gluon matrix elements of the nucleons, these

operators are numerically of similar size, or dominant. We compute each of the operator coefficients in Eq. (6) to leading order in electroweak couplings, and hence we neglect one-loop diagrams involving c_H for quark matching and two-loop diagrams involving c_H for gluon matching. The impact of higher order contributions is estimated in the numerical analysis by varying the factorization scale. The techniques for electroweak scale matching detailed in Ref. [24] can be applied to the present calculation. We describe some pertinent details here. Compared to the leading power analysis considered in Ref. [24], computation of the $1/M$ corrections requires an extended master integral basis, and different components of the electroweak polarization tensor for the background field gluon matching.

In performing the gluon matching, it is convenient to distinguish between amplitudes with one or two bosons exchanged in the t-channel. One-boson exchange amplitudes are shown in the top row of Fig. 3, while two-boson exchange amplitudes are shown in the bottom row. The one-boson exchange amplitudes factorize into the one-boson exchange amplitudes for quark matching (top row of Fig. 2) times the quark loop, and contribute only to the scalar coefficient. For the two-boson exchange amplitudes, we employ electroweak polarization tensors, $\Pi^{\mu\nu}$, induced by a loop of quarks in a background field of external gluons [24, 32, 33]. The temporal components, $v_\mu v_\nu \Pi^{\mu\nu}$, are sufficient for the leading power analysis, while for the $1/M$ corrections we require also the spatial components; these may be extracted from Ref. [24]. The renormalization of Wilson coefficients for the quark and gluon operators is discussed in Ref. [25].

From the sum of one and two loop diagrams in Figs. 2 and 3, we obtain the final results for coefficients renormalized in the $\overline{\rm MS}$ scheme:

$$
\begin{aligned}
\hat{c}_U^{(0)}(\mu) &= -\frac{1}{x_h^2} - \frac{m_W}{\pi M}\frac{c_H}{\alpha_2^2 x_h^2}\,,\\
\hat{c}_D^{(0)}(\mu) &= -\frac{1}{x_h^2} - \delta_{Db}\frac{x_t}{4(x_t+1)^3} - \frac{m_W}{\pi M}\frac{c_H}{\alpha_2^2 x_h^2}\,,\\
\hat{c}_g^{(0)}(\mu) &= \frac{\alpha_s}{4\pi}\left[\frac{1}{3x_h^2} + \frac{N_\ell}{6} + \frac{1}{6(x_t+1)^2} + \frac{m_W}{\pi M}\frac{c_H}{3\alpha_2^2 x_h^2}\right],\\
\hat{c}_U^{(2)}(\mu) &= \frac{2}{3} - \frac{m_W}{\pi M}\,,\\
\hat{c}_D^{(2)}(\mu) &= \frac{2}{3} + \delta_{Db}\left[\frac{3x_t+2}{3(x_t+1)^3} - \frac{2}{3}\right] + \frac{m_W}{\pi M}\left(-1 + \delta_{Db}\left[\frac{-x_t^2 + x_t^6 - 4x_t^4\log x_t}{(x_t^2-1)^3}\right]\right),\\
\hat{c}_g^{(2)}(\mu) &= \frac{\alpha_s}{4\pi}\left\{N_\ell\left(-\frac{16}{9}\log\frac{\mu}{m_W} - 2\right) - \frac{4(2+3x_t)}{9(1+x_t)^3}\log\frac{\mu}{m_W(1+x_t)}\right.\\
&\quad - \frac{4(12x_t^5 - 36x_t^4 + 36x_t^3 - 12x_t^2 + 3x_t - 2)}{9(x_t-1)^3}\log\frac{x_t}{1+x_t} - \frac{8x_t(-3+7x_t^2)}{9(x_t^2-1)^3}\log 2\\
&\quad - \frac{48x_t^6 + 24x_t^5 - 104x_t^4 - 35x_t^3 + 20x_t^2 + 13x_t + 18}{9(x_t^2-1)^2(1+x_t)}\\
&\quad + \frac{m_W}{\pi M}\left[N_\ell\left(\frac{8}{3}\log\frac{\mu}{m_W} - \frac{1}{3}\right) + \frac{16x_t^4}{3(x_t^2-1)^3}\log x_t\log\frac{\mu}{m_W} - \frac{4(3x_t^2-1)}{3(x_t^2-1)^2}\log\frac{\mu}{m_W} + \frac{16x_t^2}{3}\log^2 x_t\right.\\
&\quad - \frac{4(4x_t^6 - 16x_t^4 + 6x_t^2 + 1)}{3(x_t^2-1)^3}\log x_t + \frac{8x_t^2(x_t^6 - 3x_t^4 + 4x_t^2 - 1)}{3(x_t^2-1)^3}{\rm Li}_2(1-x_t^2) + \frac{4\pi^2 x_t^2}{9}\\
&\quad \left.\left. - \frac{8x_t^4 - 7x_t^2 + 1}{3(x_t^2-1)^2}\right]\right\}.
\end{aligned}
\tag{8}
$$

Here we introduce the shorthand notation $c_i = (\pi\alpha_2^2/m_W^3)\hat{c}_i$ for the effective operator coefficients, $x_i = m_i/m_W$ for masses expressed in units of m_W, and $N_\ell = 2$ is the number of massless Standard Model generations. The leading power results, represented by $M \to \infty$ in Eq. (8), were obtained in Ref. [22].[2]

[2] In obtaining the results (8), it is important to evaluate all integrals and bare coefficients in $d = 4-2\epsilon$ dimensions [22, 24].

Let us remark that our results (8) obey the correct formal limit at small x_t: [22]

$$c_g^{(0)}|_{x_t\to 0} = c_g^{(0)}(n_f=6) - \frac{\alpha_s}{12\pi} c_q^{(0)}(n_f=6) + \mathcal{O}(\alpha_s^2)\,,$$
$$c_g^{(2)}|_{x_t\to 0} = c_g^{(2)}(n_f=6) - \frac{\alpha_s}{3\pi}\log\frac{m_t}{\mu} c_q^{(2)}(n_f=6) + \mathcal{O}(\alpha_s^2)\,, \tag{9}$$

where $c(n_f=6)$ denotes the coefficient in six-flavor QCD computed with three massless generations (i.e., $m_t \ll m_W$).[3] At large x_t, $m_t \gg m_W$, the top quark contributions to the coefficients are of order $\sim m_W^2/m_t^2$. For the special case of a Majorana fermion ($c_H = -3\alpha_2^2$), the $1/M$ corrections for $c_{q,g}^{(0)}$ and $c_q^{(2)}$ are reproduced by an expansion of expressions in Ref. [35]. However, already at leading power the expression in Ref. [35] for $c_g^{(2)}$ disagrees with the corresponding results in Ref. [22] and Eq. (8). We note that the expression for $c_g^{(2)}$ in Ref. [35] does not have the correct $m_t \to 0$ limit.

4 Cross sections

Let us consider the standard benchmark process for direct detection: the zero velocity limit of (spin-independent) WIMP-nucleon scattering. The cross section is determined by the spin-0 and spin-2 matrix elements, $\mathcal{M}_N^{(0)}$ and $\mathcal{M}_N^{(2)}$, of the operators in Eq. (7),

$$\mathcal{M}_N^{(S)} = \sum_{i=q,g} c_i^{(S)}(\mu_0)\langle N|O_i^{(S)}(\mu_0)|N\rangle\,. \tag{10}$$

In order to evaluate the hadronic matrix elements using available lattice QCD calculations, the five flavor QCD theory must be matched to the appropriate three or four flavor theory, accounting for heavy quark threshold matching corrections and renormalization group evolution from electroweak to hadronic scales. Details of this matching can be found in Ref. [25]. For definiteness, we match to the three flavor theory with NNNLO QCD corrections,[4] and following Ref. [25] make the default scale choices $\mu_t = (m_t + m_W)/2 = 126\,\text{GeV}$, $\mu_b = 4.75\,\text{GeV}$, $\mu_c = 1.4\,\text{GeV}$, and $\mu_0 = 1.2\,\text{GeV}$. The impact of higher order perturbative QCD corrections is estimated by varying factorization scales $m_W^2/2 \le \mu_t^2 \le 2m_t^2$, $m_b^2/2 \le \mu_b^2 \le 2m_b^2$, $m_c^2/2 \le \mu_c^2 \le 2m_c^2$, and $1.0\,\text{GeV} \le \mu_0 \le 1.4\,\text{GeV}$. There are additional uncertainties associated with the hadronic form factors that characterize the overlap between the nucleon states and the quark and gluon operators. We employ the form factor central values and uncertainties from Ref. [25]. Errors from all sources are added in quadrature to obtain the total cross section error.

Neglecting numerically small CKM factors and isospin violation in nucleon matrix elements [25], the cross sections for scattering on protons or neutrons are identical:

$$\sigma_p \approx \sigma_n = \frac{m_r^2}{\pi}|\mathcal{M}_p^{(0)} + \mathcal{M}_p^{(2)}|^2\,, \tag{11}$$

where $m_r = m_p M/(m_p+M) \approx m_p$ is the reduced mass of the WIMP-nucleon system. In Fig. 4 we show the cross section including first order power corrections as a function of M for a fundamental fermion, Eq. (3), and for a composite scalar, Eq. (5). The central value amplitudes, in units with $\mathcal{M}_p^{(2)}|_{M\to\infty} = 1$, are

$$\mathcal{M}_p^{(2)} = 1 - 0.52\frac{m_W}{M}\,, \qquad \mathcal{M}_p^{(0)} = -0.81 - 0.50\frac{c_H}{3\alpha_2^2}\frac{m_W}{M}\,. \tag{12}$$

For a related discussion see Ref. [34].

[3] In particular, the quark matching coefficients are $\hat{c}_q^{(0)}(n_f=6) = -\frac{1}{x_h^2} - \frac{m_W}{\pi M}\frac{c_H}{\alpha_2^2 x_h^2}$ and $\hat{c}_q^{(2)}(n_f=6) = \frac{2}{3} - \frac{m_W}{\pi M}$ for $q = u,d,c,s,t,b$. The gluon matching coefficients are obtained by omitting the top quark loop contributions in Eq. (8) and setting $N_\ell = 3$: $\hat{c}_g^{(0)}(n_f=6) = \frac{\alpha_s}{8\pi}$ and $\hat{c}_g^{(2)}(n_f=6) = \frac{\alpha_s}{4\pi}\left[-\frac{16}{3}\log\frac{\mu}{m_W} - 6 + \frac{m_W}{\pi M}\left(8\log\frac{\mu}{m_W} - 1\right)\right]$.

[4] For the leading power analysis, this corresponds to amplitude "5" discussed in Figure 2 and Section 6.2.3 of Ref. [25].

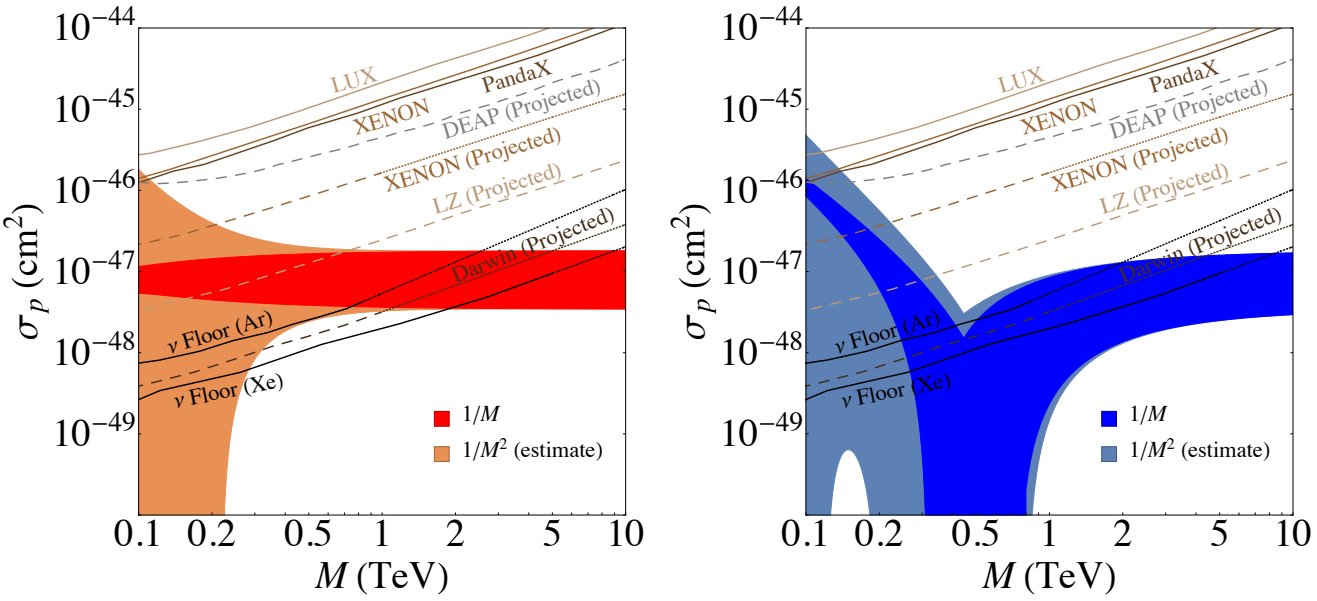

Figure 4: The WIMP-proton scattering cross section as a function of WIMP mass M for a Majorana WIMP (left panel) and a scalar WIMP (right panel), which correspond to the c_H values in Eqs. (3) and (5), respectively. The inner band is the cross section obtained from the scalar and tensor amplitudes computed through $\mathcal{O}(1/M)$. The outer band includes an estimate for the $\mathcal{O}(1/M^2)$ contributions. The neutrino floor for both Argon and Xenon direct detection experiments are from Ref. [36], and are shown by black solid lines; our extrapolation to larger masses is denoted with black dashed lines. Also shown with solid lines are the current bounds from LUX [37], XENON1T [38], and PandaX-II [39]. Projected sensitivities of future experiments are shown with dotted lines: DEAP-3600 [40], XENON1T [41], LZ [42], and DARWIN [43].

The numerical evaluation (12) exhibits the partial cancellation of the universal $M \to \infty$ result. For the Majorana fermion case, where $c_H = -3\alpha_2^2$, the m_W/M power correction also exhibits a surprising cancellation. The impact of neglected higher-order power corrections is estimated by including an uncertainty in the tensor amplitude as $\mathcal{M}_p^{(2)} \propto \mathcal{M}_p^{(2)}|_{M\to\infty}\left[1 \pm (m_W/M)^2\right]$. At large mass, the power corrections vanish, and the universal result with central value and uncertainty from Ref. [25] is reproduced. At finite WIMP mass, the dependence of the cross section on the Higgs coupling c_H differentiates the fermion and scalar cases.

Figure 4 compares to existing limits from LUX [37], XENON1T [38], and PandaX-II [39],[5] and to projected sensitivities for the Xenon based experiments XENON1T [41], LZ [42], and DARWIN [43], and the Argon based experiment DEAP-3600 [40]. Also shown is the "discovery limit" for both Xenon and Argon due to neutrino backgrounds, taken from Ref. [36].

5 Summary

The scattering of atomic nuclei from approximately static sources of electroweak SU(2) is a well posed but intricate field theory problem that finds application in the search for WIMP dark matter in our local halo. LHC bounds have pushed the scale of new physics into a regime of large mass where direct detection is more challenging; however at the same time, universal predictions emerge in this regime and provide well-defined targets for next generation searches.

[5] For masses larger than the ranges reported in these references, we have displayed an extrapolation assuming simple scaling with the WIMP number abundance, $\sigma_{\rm limit} \propto M$.

Generic amplitude level cancellations imply a potentially enhanced sensitivity of direct detection rate predictions to naively power suppressed interactions. In this paper we considered the general framework to analyze these power corrections, and analyzed the canonical case of a self-conjugate electroweak-triplet WIMP through order $1/M$. Owing to heavy particle universality, the leading cross section prediction is identical whether such a WIMP is fermion or scalar, elementary or composite, and whether the WIMP is accompanied by other, heavier, particles in the Standard Model extension. Power corrections differentiate these scenarios, as illustrated in Fig. 4 for the benchmark low-velocity WIMP-nucleon cross section. For the elementary fermion case, two contributions to the power correction largely cancel, resulting in a small deviation from the universal $M \to \infty$ limit. Our result represents the most complete calculation of the cross section for wino-like dark matter in the TeV regime. A standard thermal cosmology, consistent with the observed dark matter abundance, predicts $M \sim 2 - 3\,\text{TeV}$ for such electroweak charged WIMPs [44–48]. The elementary Majorana fermion case involves no free parameters, and a prediction $M \approx 2.9\,\text{TeV}$ is obtained after careful accounting for nonperturbative enhancements [49]. For the scalar case, the precise annihilation cross section, and hence cosmological mass constraint, depends on internal structure. At the TeV mass scales indicated by cosmological arguments, the predicted WIMP-nucleus scattering rate is comparable to the rate for neutrino-induced backgrounds. This cross section benchmark motivates very large scale detectors, and techniques to probe into the so-called neutrino floor [50].

A number of investigations are suggested by our results. Besides its computational power, the heavy WIMP expansion provides an excellent classification scheme for WIMP direct detection in the increasingly important heavy WIMP regime. The SU(2) triplet (i.e., wino-like) case represents a canonical benchmark. Other quantum numbers such as the higgsino-like case may be similarly investigated. The proximity of the triplet cross section in Fig. 4 to the neutrino floor makes the precise WIMP mass of particular interest. For the composite scalar case, new nonperturbative physics enters in two key places: the Higgs coupling parameter c_H that determines the size of the direct detection cross section; and the annihilation process that determines the cosmological mass constraint within a specified cosmological model. This physics could be accessed by lattice field theory [51] and/or chiral lagrangian analysis for the new strongly coupled sector. Two-body nuclear effects could potentially have differing impacts on the spin-0 and spin-2 operators in Eq. (6). Like the $1/M$ corrections, the existence of a severe cancellation in the leading cross section can potentially enhance the impact of such naively subleading effects. Existing estimates for such nuclear effects, focused on the spin-0 sector, indicate a small impact relative to other uncertainties [52, 53], however a more systematic analysis is warranted.

Acknowledgements

CYC would like to thank C. Burgess for helpful discussions. RJH thanks TRIUMF and Perimeter Institute for hospitality. Work of MPS was supported by the Office of High Energy Physics of the U.S. DOE under Contract Numbers DE-AC02-05CH11231 and DE-SC0011632. Research at the Perimeter Institute is supported in part by the Government of Canada through NSERC and by the Province of Ontario through MEDT. TRIUMF receives federal funding via a contribution agreement with the National Research Council of Canada. Fermilab is operated by Fermi Research Alliance, LLC under Contract No. DE-AC02-07CH11359 with the United States Department of Energy.

References

[1] "ATLAS SUSY Searches - 95% CL Lower Limits," https://atlas.web.cern.ch/Atlas/GROUPS/PHYSICS/CombinedSummaryPlots/SUSY/ATLAS_SUSY_Summary/ATLAS_SUSY_Summary.pdf (2017), accessed: 2017-09-22.

[2] "ATLAS Exotics Searches - 95% CL Lower Limits," https://atlas.web.cern.ch/Atlas/GROUPS/

PHYSICS/CombinedSummaryPlots/EXOTICS/ATLAS_Exotics_Summary/ATLAS_Exotics_Summary.pdf (2017), accessed: 2017-09-22.

[3] "Selected CMS SUSY Searches," https://twiki.cern.ch/twiki/pub/CMSPublic/PhysicsResultsSUS/Moriond2017_BarPlot.pdf (2017), accessed: 2017-09-22.

[4] "CMS Exotica Physics Group Summary," https://twiki.cern.ch/twiki/pub/CMSPublic/PhysicsResultsCombined/exo-limits_LHCP_2016.pdf (2016), accessed: 2017-09-22.

[5] G. Aad *et al.* (ATLAS), Phys. Rev. **D88**, 112006 (2013), arXiv:1310.3675 [hep-ex].

[6] V. Khachatryan *et al.* (CMS), JHEP **01**, 096 (2015), arXiv:1411.6006 [hep-ex].

[7] M. Cirelli, F. Sala, and M. Taoso, JHEP **10**, 033 (2014), [Erratum: JHEP01,041(2015)], arXiv:1407.7058 [hep-ph].

[8] M. Low and L.-T. Wang, JHEP **08**, 161 (2014), arXiv:1404.0682 [hep-ph].

[9] T. Golling *et al.*, CERN Yellow Report , 441 (2017), arXiv:1606.00947 [hep-ph].

[10] *Search for long-lived charginos based on a disappearing-track signature in pp collisions at* $\sqrt{s} = 13$ *TeV with the ATLAS detector*, Tech. Rep. ATLAS-CONF-2017-017 (CERN, Geneva, 2017).

[11] J. Hisano, S. Matsumoto, and M. M. Nojiri, Phys. Rev. Lett. **92**, 031303 (2004), arXiv:hep-ph/0307216 [hep-ph].

[12] T. Cohen, M. Lisanti, A. Pierce, and T. R. Slatyer, JCAP **1310**, 061 (2013), arXiv:1307.4082 [hep-ph].

[13] J. Fan and M. Reece, JHEP **10**, 124 (2013), arXiv:1307.4400 [hep-ph].

[14] A. Hryczuk, I. Cholis, R. Iengo, M. Tavakoli, and P. Ullio, JCAP **1407**, 031 (2014), arXiv:1401.6212 [astro-ph.HE].

[15] M. Bauer, T. Cohen, R. J. Hill, and M. P. Solon, *Proceedings, Meeting of the APS Division of Particles and Fields (DPF 2015): Ann Arbor, Michigan, USA, 4-8 Aug 2015*, JHEP **01**, 099 (2015), arXiv:1409.7392 [hep-ph].

[16] J. Bramante, P. J. Fox, G. D. Kribs, and A. Martin, Phys. Rev. **D94**, 115026 (2016), arXiv:1608.02662 [hep-ph].

[17] M. Baryakhtar, J. Bramante, S. W. Li, T. Linden, and N. Raj, Phys. Rev. Lett. **119**, 131801 (2017), arXiv:1704.01577 [hep-ph].

[18] R. Krall and M. Reece, (2017), arXiv:1705.04843 [hep-ph].

[19] M. Baumgart, I. Z. Rothstein, and V. Vaidya, Phys. Rev. Lett. **114**, 211301 (2015), arXiv:1409.4415 [hep-ph].

[20] G. Ovanesyan, T. R. Slatyer, and I. W. Stewart, Phys. Rev. Lett. **114**, 211302 (2015), arXiv:1409.8294 [hep-ph].

[21] M. Baumgart, T. Cohen, I. Moult, N. L. Rodd, T. R. Slatyer, M. P. Solon, I. W. Stewart, and V. Vaidya, (2017), arXiv:1712.07656 [hep-ph].

[22] R. J. Hill and M. P. Solon, Phys. Lett. **B707**, 539 (2012), arXiv:1111.0016 [hep-ph].

[23] R. J. Hill and M. P. Solon, Phys. Rev. Lett. **112**, 211602 (2014), arXiv:1309.4092 [hep-ph].

[24] R. J. Hill and M. P. Solon, Phys. Rev. **D91**, 043504 (2015), arXiv:1401.3339 [hep-ph].

[25] R. J. Hill and M. P. Solon, Phys. Rev. **D91**, 043505 (2015), arXiv:1409.8290 [hep-ph].

[26] J. Hisano, K. Ishiwata, N. Nagata, and T. Takesako, JHEP **07**, 005 (2011), arXiv:1104.0228 [hep-ph].

[27] A. Berlin, D. S. Robertson, M. P. Solon, and K. M. Zurek, Phys. Rev. **D93**, 095008 (2016), arXiv:1511.05964 [hep-ph].

[28] J. Heinonen, R. J. Hill, and M. P. Solon, Phys. Rev. **D86**, 094020 (2012), arXiv:1208.0601 [hep-ph].

[29] M. E. Luke and A. V. Manohar, Phys. Lett. **B286**, 348 (1992), arXiv:hep-ph/9205228 [hep-ph].

[30] C. Kilic, T. Okui, and R. Sundrum, JHEP **02**, 018 (2010), arXiv:0906.0577 [hep-ph].

[31] Y. Bai and R. J. Hill, Phys. Rev. **D82**, 111701 (2010), arXiv:1005.0008 [hep-ph].

[32] V. A. Novikov, M. A. Shifman, A. I. Vainshtein, and V. I. Zakharov, Fortsch. Phys. **32**, 585 (1984).

[33] J. Hisano, K. Ishiwata, and N. Nagata, Phys. Rev. **D82**, 115007 (2010), arXiv:1007.2601 [hep-ph].

[34] S. Weinzierl, Mod. Phys. Lett. **A29**, 1430015 (2014), arXiv:1402.4407 [hep-ph].

[35] J. Hisano, K. Ishiwata, and N. Nagata, JHEP **06**, 097 (2015), arXiv:1504.00915 [hep-ph].

[36] J. Billard, L. Strigari, and E. Figueroa-Feliciano, Phys. Rev. **D89**, 023524 (2014), arXiv:1307.5458 [hep-ph].

[37] D. S. Akerib *et al.* (LUX), Phys. Rev. Lett. **118**, 021303 (2017), arXiv:1608.07648 [astro-ph.CO].

[38] E. Aprile *et al.* (XENON), (2017), arXiv:1705.06655 [astro-ph.CO].

[39] X. Cui *et al.* (PandaX-II), (2017), arXiv:1708.06917 [astro-ph.CO].

[40] P. A. Amaudruz *et al.* (DEAP-3600), (2017), arXiv:1707.08042 [astro-ph.CO].

[41] E. Aprile (XENON1T), *Proceedings, 10th UCLA Symposium on Sources and Detection of Dark Matter and Dark Energy in the Universe: Marina de Rey, California, February 22-24, 2012*, Springer Proc. Phys. **148**, 93 (2013), arXiv:1206.6288 [astro-ph.IM].

[42] D. S. Akerib *et al.* (LZ), (2015), arXiv:1509.02910 [physics.ins-det].

[43] J. Aalbers *et al.* (DARWIN), JCAP **1611**, 017 (2016), arXiv:1606.07001 [astro-ph.IM].

[44] J. Hisano, S. Matsumoto, M. M. Nojiri, and O. Saito, Phys. Rev. **D71**, 063528 (2005), arXiv:hep-ph/0412403 [hep-ph].

[45] J. Hisano, S. Matsumoto, M. Nagai, O. Saito, and M. Senami, Phys. Lett. **B646**, 34 (2007), arXiv:hep-ph/0610249 [hep-ph].

[46] M. Cirelli, A. Strumia, and M. Tamburini, Nucl. Phys. **B787**, 152 (2007), arXiv:0706.4071 [hep-ph].

[47] A. Hryczuk, R. Iengo, and P. Ullio, JHEP **03**, 069 (2011), arXiv:1010.2172 [hep-ph].

[48] A. Hryczuk and R. Iengo, JHEP **01**, 163 (2012), [Erratum: JHEP06,137(2012)], arXiv:1111.2916 [hep-ph].

[49] M. Beneke, A. Bharucha, F. Dighera, C. Hellmann, A. Hryczuk, S. Recksiegel, and P. Ruiz-Femenia, JHEP **03**, 119 (2016), arXiv:1601.04718 [hep-ph].

[50] F. Mayet *et al.*, Phys. Rept. **627**, 1 (2016), arXiv:1602.03781 [astro-ph.CO].

[51] T. Appelquist *et al.* (Lattice Strong Dynamics (LSD)), Phys. Rev. **D89**, 094508 (2014), arXiv:1402.6656 [hep-lat].

[52] V. Cirigliano, M. L. Graesser, and G. Ovanesyan, JHEP **10**, 025 (2012), arXiv:1205.2695 [hep-ph].

[53] M. Hoferichter, P. Klos, J. Menéndez, and A. Schwenk, Phys. Rev. **D94**, 063505 (2016), arXiv:1605.08043 [hep-ph].